Narazaki, Tomoko ORCID: https://orcid.org/0000-0003-4513-3432 , Isojunno, Saana ORCID: https://orcid.org/0000-0002-2212-2135 , Nowacek, Douglas P., Swift, Rene, Friedlaender, Ari S., Ramp, Christian, Smout, Sophie, Aoki, Kagari, Deecke, Volker B. ORCID: https://orcid.org/0000-0003-2781-5915 , Sato, Katsufumi and Miller, Patrick J.O. (2018) Body density of humpback whales (Megaptera novaengliae) in feeding aggregations estimated from hydrodynamic gliding performance. PLoS ONE, 13 (7). e0200287.

1    **Body density of humpback whales (*Megaptera novaengliae*) in feeding aggregations**

2    **estimated from hydrodynamic gliding performance**

3

4    Tomoko Narazaki[1, 2*], Saana Isojunno[1], Douglas P Nowacek[3¶], Rene Swift[1¶], Ari S

5    Friedlaender[4¶], Christian Ramp[1,5¶], Sophie Smout[1&], Kagari Aoki[1,2&], Volker B Deecke[6],

6    Katsufumi Sato[2&], Patrick JO Miller[1].

7

8    [1]Sea Mammal Research Unit, University of St Andrews, Fife, United Kingdom

9    [2]Atmosphere and Ocean Research Institute, University of Tokyo, Kashiwa, Chiba, Japan

10   [3]Nicholas School of the Environment and Pratt School of Engineering, Duke University

11   Marine Laboratory, Beaufort, North Carolina, United States of America

12   [4]Institute of Marine Sciences, University of California Santa Cruz, Santa Cruz, California,

13   United States of America

14   [5]Mingan Island Cetacean Study, Longue-Pointe-de-Mingan, Québec, Canada

15   [6]Department of Science, Natural Resources and Outdoor Studies, University of Cumbria,

16   Ambleside, United Kingdom

17

18   *corresponding author

19   Email: naratomoz@gmail.com

20

21   [¶]These authors contributed equally to this work

22   [&]These authors also contribute equally to this work

23

24

# Abstract

Many baleen whales undertake annual fasting and feeding cycles, resulting in substantial changes in their body condition, an important factor affecting fitness. As a measure of lipid-store body condition, tissue density of a few deep diving marine mammals has been estimated using a hydrodynamic glide model of drag and buoyancy forces. Here, we applied the method to shallow-diving humpback whales (*Megaptera novaeangliae*) in North Atlantic and Antarctic feeding aggregations. High-resolution 3-axis acceleration, depth and speed data were collected from 24 whales. Measured values of acceleration during 5 s glides were fitted to a hydrodynamic glide model to estimate unknown parameters (tissue density, drag term and diving gas volume) in a Bayesian framework. Estimated species-average tissue density ($1031.6 \pm 2.1$ kg m$^{-3}$, $\pm 95\%$ credible interval) indicates that humpback whale tissue is typically negatively buoyant although there was a large inter-individual variation ranging from 1025.2 to 1043.1 kg m$^{-3}$. The precision of the individual estimates was substantially finer than the variation across different individual whales, demonstrating a progressive decrease in tissue density throughout the feeding season and comparably high lipid-store in pregnant females. The drag term ($C_D A m^{-1}$) was estimated to be relatively high, indicating a large effect of lift-related induced drag for humpback whales. Our results show that tissue density of shallow diving baleen whales can be estimated using the hydrodynamic gliding model, although cross-validation with other techniques is an essential next step. This method for estimating body condition is likely to be broadly applicable across a range of aquatic animals and environments.

## Introduction

The body condition of animals influences survival rate and reproductive success and thereby impacts the dynamics of entire populations. Body condition also affects an animal's behavioural decisions related to foraging, predator avoidance, migration, and reproductive strategies (e.g. [1-3]). Many marine mammals undergo substantial changes in lipid-store body condition as a result of annual fasting and feeding cycles [4, 5]. For migratory species, the cost of reproduction at breeding grounds is supported by energy gained on feeding grounds. Thus, the amount of energy stored during a feeding season strongly influences reproduction via pregnancy rate [6], foetal development [7], body condition and survival of offspring [8-11] and the competitive capabilities of males. It is also likely that body condition influences the foraging decisions made by baleen whales relative to where prey items are located in the water column [12, 13]. Because body condition is an important factor affecting fitness, measuring body condition of free-ranging cetaceans is important for understanding their ecology as well as for designing effective conservation plans [14-16].

Baleen whales (parvorder Mysticeti; order Cetartiodactyla) are a group of marine mammals that cycle fat stores on an annual basis, substantially changing their appearance, behaviour, and fitness [17]. Given these dramatic changes, developing methods to quantify their body condition in the field has great value. Traditional approaches to examine variations in body condition and energy store of baleen whales involved anatomical measurements that were often made in conjunction with whaling operations [4, 18, 19]. Blubber thickness of whale carcasses has been used as a proxy of body condition [4, 18, 20], since most of the energy is stored in the form of blubber [21] although a considerable amount of energy is also stored in muscle and intra-abdominal fat [4, 21]. Blubber lipid content of whale carcasses was also important in the assessment of condition of cetaceans [19]. As the thickness as well as lipid

72     content and fatty acid composition of blubber has been shown to vary across the body of

73     cetaceans, multiple-site measurements of blubber thickness are particularly useful to examine

74     total body condition cetaceans [22-24]. Many studies have investigated seasonal trends in

75     energy storage of several species of baleen whales by means of blubber thickness and

76     morphometric data, reporting that seasonal fattening varies with different sex and age classes,

77     reproductive stages, as well as prey availability [4, 6, 25].

78

79     Although carcasses have provided many insights into the physiology and body condition of

80     baleen whales, a key limitation is that temporal changes of the same individual cannot be

81     measured. Also, studies using carcasses may not be widely applicable to cetaceans because

82     they require lethal sampling or collection of samples from stranded animals or fisheries

83     bycatch. To collect blubber and other tissue samples from free-ranging cetaceans, biopsy

84     darting is commonly used where modified dart tips are delivered using a crossbow or a

85     pneumatic rifle [26]. The percentage lipid content of blubber from carcasses is considered to

86     be an informative measure of fattening [19]. However, the biopsy blubber samples may not be

87     useful to measure body condition of free-ranging cetaceans because the (1) the force of

88     darting can damage adipocytes causing lipids to be squeezed out of samples, or to seep out of

89     blubber biopsies while in seawater [27], and (2) the sample only penetrates a short distance

90     into the blubber layer. In addition, it is difficult to obtain multiple biopsy samples from a

91     whale whose blubber thickness and composition vary across the body [22-24]. Visual

92     assessment of external shape and appearance based on boat-based photographs has been used

93     for evaluating body condition of right and grey whales [28, 29]. Photogrammetric

94     measurements of body width, reflecting blubber thickness, using vertical aerial photographs

95     taken from aircraft or unmanned aerial vehicles has also been used to assess nutritive body

96     condition of some whale species [11, 30, 31] although measurements of such body shape

97  patterns are limited to the visible 2-dimensionall shape of surfacing of whales, and may not be

98  suitable for other more cryptic species.

99

100  An alternative approach is to use body density of diving animals as a proxy of lipid-store

101  body condition [32]. Lipids are less dense than seawater while other non-gas body

102  components are denser than seawater. Body composition, particularly the ratio of lipid to lean

103  tissue, therefore strongly influences body density and hence the buoyancy of diving animals

104  [5]. It has been shown that buoyancy influences swimming behaviour and energetics of diving

105  animals [33]. For instance, buoyancy forces affect stroking efforts [34, 35] and swimming

106  patterns, with more gliding occurring in the direction aided by buoyancy [15, 34, 36-39].

107

108  Buoyancy also influences gliding performance by altering vertical speeds during inactive drift

109  periods [5], prolonged glides [39] or short-duration glides [38]. This effect of buoyancy on

110  gliding performance has led to the development of tag-based methods to quantify the body

111  density of diving animals via hydrodynamic analysis. This approach was first developed for

112  free-ranging elephant seals (*Mirounga* spp.): body density was quantified by analysing the

113  vertical speed during inactive drifting periods (i.e. drift rate) at which the buoyancy force is

114  assumed to be equal to the drag force [5]. The drift dive method has proven useful for long-

115  term monitoring of body lipid-stores in elephant seals providing new insights into when and

116  where they gain or lose lipid stores [5, 40, 41]. However, use of the drift dive method is

117  limited to a few pinniped species that routinely perform drift dives (*Mirounga angustirostris*

118  [34, 42]; *M. leonina* [5, 40]; *Arctocephalus forsteri* [43]; *Cystophora cristata* [44]). Gliding

119  during the descent or ascent phase of a dive, on the other hand, is commonly observed across

120  a range of diving taxa [33, 37]. A more widely applicable approach, the glide model, was

121  introduced by Miller et al. [38] to estimate body density of sperm whales using a

122  hydrodynamic glide model that predicts how drag and buoyancy forces influence acceleration

123  (or deceleration) during short-duration glides. Aoki et al. [34] conducted a validation analysis

124  using isotope dilution and confirmed a strong correspondence in body density estimates of

125  elephant seals obtained from the drift dive and the glide models [45].

126

127  In the glide model, acceleration during a glide is determined by the difference between drag

128  and net buoyancy forces along the swimming path of the animal [38]. The force of non-

129  neutral buoyancy or 'apparent weight' (difference in mass of the diving animal and the

130  displaced water) acts vertically on diving animals, and depends on the density of body tissues

131  as well as the volume of air carried within the body (the diving gas volume). While body

132  tissues are relatively incompressible at depth, the volume of air in the body progressively

133  decreases with increasing depth, thought to closely follow Boyle's Law for marine mammals

134  [46]. Thus, tissue-derived buoyancy can be separated from air-derived buoyancy when gliding

135  data is available over a wide depth range. To date, the glide model has been demonstrated to

136  be useful to estimate the body density of several species of marine mammals, including

137  elephant seals [34] and some deep diving toothed whales (sperm whale, *Physeter*

138  *macrocephalus* [38]; Northern bottlenose whale, *Hyperoodon ampullatus* [15]; long-finned

139  pilot whale, *Globicephala melas* [47]) that routinely perform dives deeper than 200 m where

140  the effect of air-derived buoyancy is considered to be negligible [38].

141

142  In this study, we apply the hydrodynamic glide model to estimate body tissue density of

143  humpback whales (*Megaptera novaeangliae*) in two geographically distinct feeding

144  populations (the Gulf of St Lawrence, Canada and the Western Antarctic Peninsula, WAP). In

145  comparison with deeper diving toothed whales, humpback whales may not seem ideal

146  candidates for the glide model because they routinely dive only to relatively shallow depths at

147 which gas volumes are likely to more strongly influence net buoyancy. For example, the mean

148 dive depth per tag record in this study ranged from 22.8 to 180.8 m, with the deepest dive

149 recorded being 388.3 m. Apart from a shallower diving depth range, humpback whales tend to

150 dive and glide at relatively shallower pitch angles, requiring the generation of lift.  The large

151 flippers of humpback whales are well-suited for this purpose [48], but the need to generate

152 substantial lift forces may raise concerns about the applicability of the glide model because

153 the current model does not include the potential effect of lift-induced drag which was shown

154 to be negligible in deep divers that maintain steep pitch during glides [34].

155

156 The objective of this study was to examine whether the hydrodynamic glide model can be

157 applied to shallower diving baleen whales by examining the precision of body density

158 estimates obtained from a narrow depth-range dataset. Our results show that we were able to

159 obtain estimates of humpback whale body density using this method. Though the precision of

160 the estimates was not as fine as was previously reported for a deep-diving toothed whale [15],

161 the precision of individual body density estimates was substantially finer than the variation

162 across different individual whales, including some differences between the geographic

163 locations where tags were attached. We conclude that the glide method has potential to be

164 used to track the body condition of shallow diving baleen whales, enabling future applications

165 as a tool to study their health and how body condition relates to reproductive status, animal

166 behaviour and the influences of environmental change and variability.

167

168 # Materials and methods

169 ## Ethics statement

170    The research protocol was approved by Animal Welfare and Care Committee Approval of the

171    University of St Andrews. The fieldwork in the Gulf of St Lawrence, Canada was performed

172    under permits issued by the Research permits issued by Department of Fisheries and Oceans,

173    Canada (scientific fishing license QUE04-B-2011) in compliance with ethical and local use of

174    animals in experimentation. All research activities in the Antarctic was conducted under

175    National Marine Fisheries Service Permit (808-1735), Antarctic Conservation Act Permit

176    (2009-014), and Duke University Institutional Animal Care and Use Committee (A049-112-

177    02).

178

## Data collection

180    Field studies were carried out at two geographically distinct summer feeding grounds of

181    humpback whales (*Megaptera novaeangliae*): the Gulf of St Lawrence in Canada and the

182    western side of Antarctic Peninsula. Animal-borne archival tags used in the study were either

183    3MPD3GT loggers (Little Leonardo Co., Tokyo, Japan) or sound and movement recording

184    DTAGs ([49]; Table 1). The 3MPD3GT loggers were programmed to record depth,

185    temperature, flywheel swim speed and 3-axis magnetism at 1Hz, and 3-axis $\pm$ 3 *g* acceleration

186    at 32Hz. The DTAG sampled pressure and a 3-axis $\pm$ 2 *g* acceleration at 50Hz, which was

187    later downsampled to 5Hz. The 3MPD3GT loggers have the ability to measure flow speed

188    using a front mounted impeller (flywheel). To ensure that speed is measured in the direction

189    of travel, 3MPD3GT tags are mounted in hydrodynamic (tear shaped) floats with a single

190    suction cup mounted at the anterior end, and vertically mounted tail fin at the posterior end.

191    The location of fin and suction cup ensure that the force acting on the tag cause the tag

192    housing to swivel on the animal and orient into the direction of flow. DTAGs are attached to

193    the animal with four suction cups. Tagging was conducted from rigid-hull inflatable boats and

194    either a 5 m or an 8 m handheld carbon fibre pole was used to attach the tag.

**Table 1. Humpback whale dataset used for analysis.**

| Data ID | Date | Location | Duration (h) | Tag type | Age class | Sex | No of 5-s glides | $\rho_{tissue}$ (kg m$^{-1}$) | $C_D Am^{-1}$ (x10$^{-6}$ m$^2$ kg$^{-1}$) |
|---|---|---|---|---|---|---|---|---|---|
| Mn11_H584_1 | 21 Jul 2011 | GSL | 0.2 | 3MPD3GT | Adult (pregnant) | F | 0 | N/A | N/A |
| Mn11_H607_1 | 22 Jul 2011 | GSL | 3.4 | 3MPD3GT | Adult | M | 23 | 1037.0 ± 1.9 | 12.5 ± 1.4 |
| Mn11_H686 | 25 Jul 2011 | GSL | 4.5 | 3MPD3GT | Adult | F | 75 | 1036.2 ± 1.2 | 6.5 ± 2.1 |
| Mn11_H761 | 25 Jul 2011 | GSL | 5.9 | 3MPD3GT | Adult | M | 44 | 1029.0 ± 1.8 | 16.3 ± 6.5 |
| Mn11_H731 | 26 Jul 2011 | GSL | 2.7 | 3MPD3GT | Adult | F | 61 | 1035.4 ± 1.2 | 12.8 ± 2.0 |
| Mn11_H698 | 26 Jul 2011 | GSL | 2 | 3MPD3GT | Adult | M | 61 | N/A | NN/A |
| Mn11_H228 | 27 Jul 2011 | GSL | 0.2 | 3MPD3GT | Adult | F | 3 | N/A | N/A |
| Mn11_H584_2 | 28 Jul 2011 | GSL | 3.6 | 3MPD3GT | Adult (pregnant) | F | 47 | 1028.6 ± 0.7 | 12.2 ± 1.4 |
| Mn11_H707 | 19 Aug 2011 | GSL | 1.6 | 3MPD3GT | Juvenile | M | 93 | 1043.1 ± 1.6 | 12.4 ± 1.5 |
| Mn11_H755 | 28 Aug 2011 | GSL | 2.9 | 3MPD3GT | Juvenile | M | 177 | 1033.7 ± 0.5 | 25.5 ± 1.0 |
| Mn11_H607_2 | 01 Sep 2011 | GSL | 2.1 | 3MPD3GT | Adult | M | 29 | 1031.2 ± 2.3 | 15.0 ± 9.6 |
| Mn11_H002 | 04 Sep 2011 | GSL | 5.8 | 3MPD3GT | Adult (pregnant) | F | 187 | 1026.5 ± 0.5 | 6.3 ± 2.8 |
| Mn11_H405 | 18 Sep 2011 | GSL | 2.7 | 3MPD3GT | Adult | M | 74 | 1034.2 ± 0.9 | 13.1 ± 1.1 |
| Mn11_H489 | 19 Sep 2011 | GSL | 0.1 | 3MPD3GT | Adult | F | 0 | N/A | N/A |
| Mn09_121 | 01 May 2009 | A | 6.4 | Dtag | Adult | U | 7 | N/A | N/A |
| Mn09_122 | 02 May 2009 | A | 4.2 | Dtag | Adult | U | 5 | N/A | N/A |
| Mn09_127a | 07 May 2009 | A | 24.2 | Dtag | Adult | U | 290 | 1028.4 ± 0.1 | 11.7 ± 0.2 |
| Mn09_127b | 07 May 2009 | A | 6.5 | Dtag | Adult | U | 15 | N/A | N/A |
| Mn09_128 | 08 May 2009 | A | 2.4 | Dtag | Adult | U | 11 | N/A | N/A |
| Mn09_136 | 16 May 2009 | A | 22.5 | Dtag | Adult | U | 704 | 1028.7 ± 0.03 | 11.2 ± 0.2 |
| Mn09_140 | 20 May 2009 | A | 22.3 | Dtag | Adult | U | 500 | 1029.8 ± 0.04 | 9.8 ± 0.2 |
| Mn09_148 | 28 May 2009 | A | 25.5 | Dtag | Adult | U | 30 | 1026.9 ± 0.7 | 10.1 ± 2.1 |
| Mn09_151 | 29 May 2009 | A | 3.1 | Dtag | Juvenile | F | 5 | N/A | N/A |
| Mn09_152 | 01 Jun 2009 | A | 22.4 | Dtag | Adult | U | 230 | 1036.3 ± 0.4 | 10.5 ± 1.3 |
| Mn10_133 | 13 May 2010 | A | 22.8 | Dtag | Adult | F | 86 | 1028.6 ± 0.3 | 6.6 ± 2.4 |
| Mn10_139a | 19 May 2010 | A | 22.2 | Dtag | Calf of Mn10_139b | F | 118 | 1040.8 ± 0.5 | 14.7 ± 0.9 |
| Mn10_139b | 19 May 2010 | A | 23.7 | Dtag | Adult | F | 457 | 1029.4 ± 0.1 | 17.4 ± 1.5 |
| Mn10_143 | 23 May 2010 | A | 23.3 | Dtag | Unknown | U | 77 | 1026.4 ± 0.3 | 22.3 ± 3.1 |

| Mn10_144 | 24 May 2010 | A | 19.9 | Dtag | Adult | M | 47 | 1031.1 ± 0.9 | 6.0 ± 3.5 |
|---|---|---|---|---|---|---|---|---|---|
| Mn10_146 | 26 May 2010 | A | 20.2 | Dtag | Adult | F | 419 | 1029.7 ± 0.1 | 11.6 ± 0.1 |
| Mn10_151 | 31 May 2010 | A | 25 | Dtag | Juvenile | F | 352 | 1035.3 ± 0.2 | 14.0 ± 0.5 |
| Mn10_155a | 04 Jun 2010 | A | 24.2 | Dtag | Adult | F | 391 | 1027.6 ± 0.1 | 14.1 ± 0.3 |
| Mn10_155b | 04 Jun 2010 | A | 22 | Dtag | Calf of Mn10_155a | F | 67 | 1025.2 ± 0.4 | 12.8 ± 1.9 |

197 GSL and A in the Location column indicate Gulf of St. Lawrence and Antarctica, respectively. Individual-specific estimates of tissue density

198 ($\rho_{tissue}$) and the combined drag term ($C_DAm^{-1}$) obtained from the lowest DIC model are presented as mean ± 95% credible interval. Data was not

199 used for the Bayesian estimation when number of 5-s glides was < 20. Dataset shaded with grey were not used for the Bayesian estimation due to

200 insufficient number of 5-s glides in the dataset.

201

## Analysis of tag data

202

203 Pressure data recorded by archival tags were converted to absolute values of hydrostatic

204 pressure using calibration values and converted to meters. A dive was defined as any

205 submergence to a depth of > 10 m. Dives were broken into descent, bottom and ascent phases

206 based on changes in pitch following Miller *et al.* [38]. As tags were attached to whales at

207 random orientations, the 3-axis acceleration data recorded by the tags was converted to a

208 whale-centred, whale fixed reference frame (whale-frame) using established methods [38,

209 49]. The accelerometers recorded both specific (e.g. stroking) and gravity-based accelerations

210 (i.e. changes in response to posture change). Under the assumption that changes in the posture

211 of the tagged whale occurred at lower frequency than changes in accelerations resulting from

212 body motions such as thrust, a frequency-based filter (low-pass finite impulse response filters

213 with tag-specific thresholds set at 0.12 – 0.15 Hz) was applied to the entire acceleration time-

214 series to separate these two components. Then, pitch and roll angles of the whales were

215 calculated from the low-frequency component of accelerations [37, 39, 50], while the high-

216 frequency component was used to identify stroking versus gliding periods. For 3MPD3GT

217 dataset, stroking was identified when oscillation on the high-frequency component of surge

218 accelerations indicating fluke beats exceeded a threshold that was set for each deployment

219 (0.1 – 0.2 m s$^{-2}$). Speed sensor data was visually inspected to confirm the presence of stroke-

220 derived acceleration. For DTAG dataset, stroking was detected using high-frequency

221 accelerations at both surge and dorso-ventral axis with thresholds set for each deployment and

222 each axis (0.1 – 0.2 m s$^{-2}$). Gliding periods were automatically detected as the period when

223 the tagged animals did not stroke.

224

225 The speed sensor of the 3MPD3GT logger recorded swim speed as the rotation of an external

226 impeller mounted on the anterior end of the logger, which correlates linearly with the speed of

227  water flow passing through the impeller. The rotation rate (number of rotations per second)

228  was converted to speed (m s$^{-1}$) using a calibration line obtained in-situ for each deployment

229  [37]. The calibration line was obtained from a linear regression of rotation rate against swim

230  speed that  was calculated from vertical depth change divided by sine of the pitch at 5 s

231  intervals when absolute mean sine of pitch was greater than 0.7 - 0.9. For the DTAG data,

232  speed during glides was estimated using the rate of change of depth divided by the sine of

233  pitch [38].

234

235  Data during glides were extracted in 5 s duration segments [15]. Glides shorter than 5 s were

236  excluded from the analysis and glides longer than 5 s were broken into 5 s sub-glides. For

237  each 5 s sub-glide, mean depth ($d$), speed ($v$) and pitch angle ($p$) were calculated. Acceleration

238  ($a$) was measured by regressing speed versus time over each 5-second interval (Fig. S1). The

239  variance of the acceleration measurement during each 5 s sub-glide was quantified as the root

240  mean square of residuals from the fitted regression line. Seawater density ($\rho_{sw}$) for each sub-

241  glide was calculated from a CTD cast that was made close in time and location to each tagged

242  whale. In this analysis, we only used stable glides (circular variance of roll < 0.1) that were at

243  steep pitch angle (absolute pitch > 30°) to enable robust estimates of speed for DTAG records.

244  In addition, any glides associated with lunge feeding were excluded from the analysis because

245  body form and kinematics of whales drastically change during this feeding behaviour [51].

246  Lunge feeding events were detected as peaks in jerk (i.e. differential of acceleration) for

247  DTAG records [52]. For 3MPD3GT records with speed data, a lunge was detected as peak in

248  speed when the speed exceeded the threshold of mean speed plus two standard deviations

249  followed by a rapid deceleration.  According to a fine-scale kinematic study of lunge-feeding

250  humpback whales, whales stroke throughout lunges but glide at the end of feeding once the

251  mouth has been closed [52]. To exclude any feeding-related glides, we excluded any glides

252 recorded within 46 s after the lunge from the analysis because it has been reported that

253 humpback whales spend an average of 46 s for filtration and prey handling [52].

254

## Hydrodynamic performance model

256 We used the equation presented by Miller *et al.* [15] where acceleration (m s$^{-2}$) along the

257 swimming path is determined by drag force (the first term) and buoyancy forces derived from

258 body tissue (the second term) and gasses carried by each whale (the third term):

259 $\text{Acceleration} = -0.5 \cdot \frac{C_D \cdot A}{m} \cdot \rho_{sw} \cdot v^2 + \left( \frac{\rho_{sw}}{\rho_{tissue}(d)} - 1 \right) \cdot g \cdot \sin(p)$

$$+ \frac{V_{air}}{m} \cdot g \cdot \sin(p) \cdot \frac{\rho_{sw} - \rho_{air} \cdot (1 + 0.1 \cdot d)}{(1 + 0.1 \cdot d)}$$

260 where:

261 $$\rho_{tissue}(d) = \frac{\rho_{tissue}(0)}{1 - r \cdot (1 + 0.1 \cdot d) \cdot 101325 \cdot 10^{-9}}$$

262

263 Here, $C_D$ is the drag coefficient, $A$ is the relevant surface area (m$^2$), $m$ is the mass of the whale

264 (kg), $\rho_{sw}$ is the density of the surrounding seawater (kg m$^{-3}$), $v$ is swim speed (m s$^{-1}$), $\rho_{tissue}$ is

265 the density of the non-gas component of the whale body (kg m$^{-3}$), $g$ is acceleration due to

266 gravity (9.8 m s$^{-2}$), $p$ is animal pitch (radians), $V_{air}$ is the volume of air at the surface (m$^3$), $\rho_{air}$

267 is the density of air (kg m$^{-3}$), $d$ is glide depth (m), and $r$ is compressibility for animal tissue

268 (i.e., the fractional change in volume per unit increase in pressure). The value 101325

269 converts pressure in atmospheres to pressure in Pascals, so that the units of body tissue

270 compressibility are proportion per Pascal x 10$^{-9}$.

271

272 The first additive term of the equation represents the effect of drag on the forward motion of

273 the whale during a glide, which is primarily a function of speed itself. $C_D A m^{-1}$ is the unknown

274 term that is treated as a single quantity in this approach with units of m$^2$ kg$^{-1}$. The second term

275    quantifies the effect of net buoyancy derived from unknown tissue density ($\rho_{sw}$) on speed

276    during a glide. The third term quantifies the influence of net buoyancy derived from the

277    unknown volume of gas per unit mass carried in the dive ($V_{air}m^{-1}$) on speed during a glide. As

278    gas compartments of whales are compressed during dives, the volume and density of gas

279    carried by the animal are modelled to change with hydrostatic pressure following Boyle's

280    Law. The model also includes the effect of tissue compressibility ($r$) that was fixed as 0.38 x

281    $10^{-9}$ $Pa^{-1}$ based on the value estimated for northern bottlenose whales [15].

282

## Bayesian estimation

284    The unknown parameters in the hydrodynamic glide model (mainly $\rho_{tissue}$, $V_{air}m^{-1}$ and $C_DAm^{-1}$

285    $^{1}$) were estimated by Bayesian Gibbs sampling with the freely available software JAGS within

286    R (coda, R package v0.17-1 2015, http://cran.r.project.org/web/packages/coda/index.html)

287    and        R2jags        (R        package        v0.5-7        2012,        https://cran.r-

288    project.org/web/packages/R2jags/index.html) using data extracted for each 5-s sub-glide.

289    Acceleration during glides was measured using a linear regression line of speed versus time.

290    Observation error measured from variance of acceleration for each 5 s was incorporated in the

291    model by treating acceleration as a normal variable with a precision parameter (1/variance)

292    [15]. A small increment (0.001) was added to the standard errors to ensure finite values for

293    the precision parameter. For the Bayesian estimation, a specific prior distribution must be set

294    for each unknown parameter. A non-informative uniform prior from 800 to 1200 kg $m^{-3}$ was

295    set for body tissue density ($\rho_{tissue}$). An informative prior was set for the combined drag

296    coefficient term ($C_DAm^{-1}$) based on several sources of information: drag coefficient ($C_D$) was

297    estimated to be 0.0026 based on the value estimated for a fin whale (*Balaenoptera physalus*)

298    swimming at 4 m $s^{-1}$ [53]. Based on body lengths ($L$) ranges from 6 to 15 m, body mass ($m$)

299    was estimated as 20005 kg on average (range 3253 - 48556 kg) using an equation derived for

300    humpback whales: $m = 0.016473L^{2.95}$ x 1000 [54]. Surface area ($A$) was estimated as 47.4 m$^2$

301    (range 15.3 – 89.0 m$^2$) using a prediction equation obtained from bottlenose dolphins

302    (*Tursiops truncatus*): A = $0.08m^{0.65}$ [55]. Thus, an expected value for the combined drag term

303    ($C_DAm^{-1}$) would be 7 x 10$^{-6}$ m$^2$ kg$^{-1}$, with a range from 5 x 10$^{-6}$ m$^2$ kg$^{-1}$ for large whales to 12

304    x 10$^{-6}$ m$^2$ kg$^{-1}$ for small whales. In order to capture uncertainty around this expected value, we

305    specify the prior to be a normal distribution with a mean of 7 x 10$^{-6}$ m$^2$ kg$^{-1}$ and standard

306    deviation of 2 x 10$^{-6}$ m$^2$ kg$^{-1}$ that was truncated at 1 x 10$^{-6}$ m$^2$ kg$^{-1}$ and 20 x 10$^{-6}$ m$^2$ kg$^{-1}$. For

307    diving gas volume ($V_{air}m^{-1}$), a uniform prior from 5 to 80 ml kg$^{-1}$ was set based on the total

308    lung capacity (65 – 72 ml kg$^{-1}$) estimated for 6 to 15 m long whales using an equation derived

309    from various marine mammals: total lung capacity = $0.10m^{0.96}$ x 1000 [56].

310

311    Following Miller et al. [15], we explored variability of unknown tissue density, combined

312    drag term and diving gas volume by evaluating a total of 12 model structures. We fitted a

313    model in which the quantity of the unknown parameters $\rho_{tissue}$, $V_{air}m^{-1}$ and $C_DAm^{-1}$ remained

314    constant across the tags and dives (global estimates). We also fitted hierarchical models in

315    which the individual-specific estimates of tissue density and/or drag term, and the dive-

316    specific estimates for diving gas volume are sampled from each global (i.e. individual-average

317    or dive-average) distribution that was estimated for each parameter. See the JAGS script in

318    the appendix of Miller et al. [15] for the detailed structure of the hierarchical model. All

319    models were sampled in three independent chains, with 24,000 iterations each. The first

320    12,000 samples were discarded for burn-in, and the remaining posterior samples were

321    downsampled by a factor of 36 to remove any serial correlation in the samples. We report the

322    mean and 95% percentile, hereafter termed posterior mean and credible interval (CI), of the

323    posterior samples as the best estimates of the parameter value and its uncertainty. The 95%

324    credible interval is the Bayesian analogue for the more traditional (frequentist) confidence

325     interval, and defines the range of values within which the true parameter value lies with 95%

326     probability, given the observed data. Convergence was assessed for each parameter, using

327     trace history and Brooks-Gelman-Rubin diagnostic plots [57]. The best model was selected

328     based on the deviance information criterion (DIC), with a lower value indicating a better

329     model fit relative to model complexity.

330

# Results

332     A total of 33 tag datasets were analysed (Table 1).  In the Gulf of St Lawrence, archival tags

333     were deployed on 12 whales in the Jacques-Cartier Passage and adjacent waters between July

334     and September 2011. All tagged whales were part of a long-term photo-identification study

335     that has been carried out at the study site since 1984 [58]. Photographic and field observations

336     of behaviour and known associates suggest that at least two adult females (H002 and H584_2)

337     were pregnant when the tag data were collected. Pregnancy of H002 was also confirmed by

338     hormonal analysis of blow samples and blubber samples. One adult male (H607) was tagged

339     twice at the beginning of the feeding season (July 22, 2011) and later the same season

340     (September 1, 2011). At the Antarctic field-site, 19 whales were tagged over the course of two

341     field seasons that ran between May and June in both 2009 and 2010. Antarctic animals were

342     tagged in Wilhelmina and Andvord Bays along the WAP and inshore waters of the Gerlache

343     Strait. Two pairs of tagged whales were found to be mother-and-calf pairs based on visual

344     observation from the tag boat and biopsy samples (Table 1).The whales conducted dives to a

345     maximum depth of 388.3 m. Mean swim speed throughout dives was $1.5 \pm 0.4$ m s$^{-1}$ ($\pm$ SD,

346     Table 2).  Gliding was observed both during descent and ascent phases although the

347     percentage of time spent gliding varied among whales ranging over $1.5 - 45.2\%$ and $2.8 -$

348     60.0% during descent and ascent phases, respectively. Pitch angles during descent and ascent

349     phases were $-39.8 \pm 20.6°$ and $30.6 \pm 22.4°$ on average, respectively (Table 2). From the

whole dataset, we extracted a total of 18546 5-s sub-glides that were not associated with a lunge. However, 73.7% of these glides were filtered out due to shallow pitch angle ($< 30°$) and 0.1% due to high variability in roll (circular variance of roll $> 0.9$). In addition, 1.4% of glides were removed due to lack of speed and/or acceleration data throughout the 5-s glides. As a result, 24.7% of the total 5-s sub-glides met the criteria for the use of hydrodynamic glide model. The number of 5-s sub-glides that could be used for the hydrodynamic glide model was positively correlated with the duration of tag dataset (Spearman's rho = 0.633, p < 0.001; Fig. 1a) although the number of useable glides also varied depending on the behaviour of the tagged whales (foraging, resting, etc.). Eight tag datasets were excluded from the Bayesian estimation of tissue density because of insufficient sample size (<20 sub-glides in each dataset; Table 1). Data of Mn11_H698 was also excluded because an in-situ calibration of the speed sensor was not applicable for this deployment.
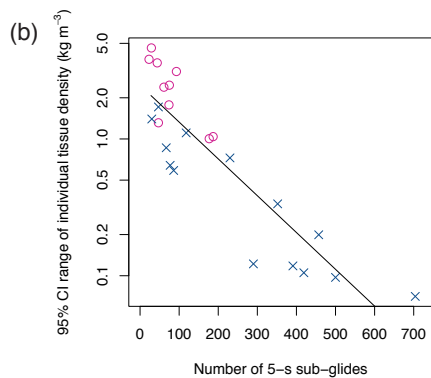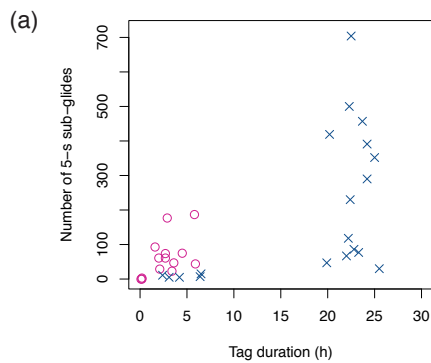
363   **Fig. 1 The number of 5-s sub-glides in relation to tag duration and 95% CI range.**

364   Number of 5-s sub-glides that could be used for the hydrodynamic glide model in relation to

365   tag duration (a) and the range of 95% credible interval for tissue density estimates (b).

366   Magenta circles and blue crosses indicate data from Gulf of St Lawrence and Antarctica,

367   respectively. A solid line shows a regression line: $\log(y) = -0.0062x + 0.90$.

368

369    **Table 2. Summary of dive statistics**

| | *Dives* | | | | *Descent phase* | | | *Ascent phase* | | |
|---|---|---|---|---|---|---|---|---|---|---|
| **Data ID** | **N** | **Duration (s)** | **Depth (m)** | **Speed (m s$^{-1}$)** | **Duration (s)** | **Pitch (°)** | **% time gliding** | **Duration (s)** | **Pitch (°)** | **% time gliding** |
| Mn11_H584_1 | 0 | N/A | N/A | N/A | N/A | N/A | N/A | N/A | N/A | N/A |
| Mn11_H607_1 | 68 | 133.1 ± 70.6 | 45.1 ± 14.4 | 2.1 ± 0.3 | 50.8 ± 24.6 | -26.0 ± 10.7 | 7.7 ± 14.4 | 42.4 ± 20.7 | 28.8 ± 8.7 | 6.0 ± 11.3 |
| Mn11_H686 | 32 | 204.7 ± 105.8 | 56.7 ± 60.7 | 1.3 ± 0.4 | 63.6 ± 47.7 | -18.1 ± 13.5 | 14.5 ± 21.0 | 85.8 ± 46.4 | 23.9 ± 24.5 | 8.8 ± 16.6 |
| Mn11_H761 | 51 | 158.4 ± 110.1 | 25.3 ± 35.7 | 1.0 ± 0.3 | 37.8 ± 26.8 | -23.4 ± 14.2 | 21.1 ± 29.5 | 91.7 ± 85.6 | 19.0 ± 13.0 | 35.1 ± 33.5 |
| Mn11_H731 | 33 | 140.9 ± 81.6 | 44.3 ± 43.6 | 1.3 ± 0.4 | 52.5 ± 37.2 | -22.0 ± 17.0 | 31.1 ± 26.9 | 67.6 ± 41.5 | 20.8 ± 10.8 | 38.1 ± 31.8 |
| Mn11_H698 | 43 | 101.1 ± 48.3 | 32.6 ± 18.5 | N/A | 25.4 ± 8.9 | -28.7 ± 16.8 | 37.3 ± 28.3 | 56.9 ± 30.1 | 20.1 ± 9.5 | 34.1 ± 26.6 |
| Mn11_H228 | 4 | 158.0 ± 85.1 | 24.9 ± 12.2 | 1.5 ± 0.5 | 38.5 ± 7.1 | -21.7 ± 11.5 | 42.5 ± 31.4 | 99.0 ± 80.4 | 13.0 ± 1.8 | 60.0 ± 41.4 |
| Mn11_H584_2 | 32 | 256.4 ± 153.1 | 70.0 ± 54.7 | 2.2 ± 0.6 | 75.6 ± 41.5 | -22.7 ± 16.8 | 5.5 ± 13.9 | 96.2 ± 73.9 | 19.2 ± 9.8 | 16.1 ± 26.2 |
| Mn11_H707 | 17 | 294.1 ± 162.5 | 116.4 ± 58.6 | 2.0 ± 0.3 | 50.1 ± 26.5 | -39.2 ± 19.0 | 45.2 ± 27.5 | 70.1 ± 30.6 | 45.7 ± 26.1 | 6.1 ± 15.4 |
| Mn11_H755 | 28 | 328.0 ± 203.0 | 73.4 ± 45.9 | 1.3 ± 0.3 | 58.7 ± 47.1 | -32.1 ± 16.4 | 37.1 ± 33.5 | 93.4 ± 66.6 | 19.8 ± 11.8 | 41.3 ± 31.2 |
| Mn11_H607_2 | 13 | 210.0 ± 107.2 | 64.2 ± 51.3 | 1.2 ± 0.3 | 65.2 ± 36.1 | -26.2 ± 19.5 | 19.9 ± 24.3 | 95.1 ± 79.1 | 21.0 ± 12.5 | 8.3 ± 17.8 |
| Mn11_H002 | 57 | 217.0 ± 107.2 | 51.9 ± 41.6 | 1.3 ± 0.3 | 63.8 ± 45.3 | -18.8 ± 9.3 | 24.8 ± 24.0 | 90.4 ± 67.0 | 15.7 ± 10.4 | 39.5 ± 31.0 |
| Mn11_H405 | 24 | 333.7 ± 194.1 | 76.6 ± 44.4 | 1.9 ± 0.3 | 70.8 ± 36.3 | -25.1 ± 12.0 | 31.9 ± 21.6 | 72.3 ± 36.9 | 25.2 ± 14.5 | 12.0 ± 11.2 |
| Mn11_H489 | 0 | N/A | N/A | N/A | N/A | N/A | N/A | N/A | N/A | N/A |
| Mn09_121 | 16 | 215.4 ± 79.0 | 48.9 ± 36.4 | 1.3 ± 0.2 | 77.0 ± 25.7 | -28.9 ± 11.6 | 23.4 ± 15.4 | 126.6 ± 56.9 | 15.1 ± 7.6 | 58.4 ± 34.1 |
| Mn09_122 | 48 | 138.6 ± 73.5 | 22.8 ± 14.2 | 1.3 ± 0.5 | 1.8 ± 27.6 | -13.0 ± 11.2 | 4.7 ± 6.3 | 67.5 ± 38.6 | 14.3 ± 7.4 | 13.4 ± 14.5 |
| Mn09_127a | 134 | 299.1 ± 216.7 | 127.5 ± 116.7 | 1.4 ± 0.4 | 93.8 ± 69.2 | -43.1 ± 20.7 | 9.4 ± 12.6 | 111.9 ± 86.8 | 38.5 ± 19.5 | 23.4 ± 22.9 |
| Mn09_127b | 29 | 211.9 ± 133.6 | 76.9 ± 71.3 | 1.8 ± 0.7 | 61.0 ± 41.5 | -35.6 ± 8.7 | 13.0 ± 15.3 | 118.6 ± 68.8 | 9.1 ± 10.8 | 56.9 ± 27.7 |
| Mn09_128 | 21 | 243.9 ± 133.9 | 32.0 ± 14.1 | 1.2 ± 0.3 | 81.1 ± 48.6 | -27.2 ± 9.6 | 13.4 ± 18.2 | 110.8 ± 71.0 | 10.3 ± 13.6 | 29.7 ± 27.3 |
| Mn09_136 | 101 | 459.3 ± 136.7 | 180.8 ± 75.9 | 1.2 ± 0.2 | 129.8 ± 51.7 | -61.6 ± 15.2 | 17.0 ± 14.5 | 159.3 ± 56.3 | 55.7 ± 20.4 | 36.8 ± 15.8 |
| Mn09_140 | 141 | 357.2 ± 181.2 | 68.8 ± 72.4 | 1.4 ± 0.4 | 89.8 ± 56.9 | -23.3 ± 14.1 | 28.5 ± 20.4 | 99.2 ± 81.1 | 20.3 ± 11.6 | 42.3 ± 25.9 |
| Mn09_148 | 308 | 127.4 ± 102.9 | 40.3 ± 34.9 | 1.6 ± 0.3 | 40.2 ± 26.9 | -37.1 ± 17.3 | 5.9 ± 10.7 | 40.3 ± 31.1 | 29.7 ± 15.3 | 14.5 ± 22.5 |
| Mn09_151 | 18 | 56.6 ± 29.5 | 175.9 ± 101.6 | 1.2 ± 0.6 | 56.6 ± 29.5 | -24.0 ± 7.8 | 37.0 ± 27.0 | 97.9 ± 71.8 | 12.3 ± 10.3 | 43.5 ± 32.2 |
| Mn09_152 | 326 | 118.1 ± 111.5 | 34.9 ± 30.4 | 1.3 ± 0.3 | 39.4 ± 34.1 | -48.0 ± 17.6 | 12.5 ± 19.7 | 34.6 ± 31.6 | 29.6 ± 12.7 | 5.3 ± 12.4 |
| Mn10_133 | 185 | 217.0 ± 99.5 | 76.1 ± 41.7 | 1.6 ± 0.3 | 72.2 ± 35.1 | -40.0 ± 15.2 | 1.5 ± 4.6 | 73.0 ± 42.1 | 32.9 ± 13.2 | 10.6 ± 13.6 |
| Mn10_139a | 288 | 170.5 ± 112.3 | 58.7 ± 38.3 | 1.5 ± 0.2 | 36.6 ± 28.4 | -53.7 ± 18.1 | 8.6 ± 17.2 | 56.1 ± 47.7 | 44.2 ± 15.0 | 8.5 ± 15.0 |
| Mn10_139b | 285 | 172.1 ± 100.3 | 45.8 ± 39.3 | 1.2 ± 0.3 | 58.6 ± 35.0 | -33.0 ± 15.0 | 7.0 ± 13.5 | 70.5 ± 53.2 | 25.5 ± 14.5 | 22.3 ± 27.1 |

20

| | | | | | | | | | | |
|---|---|---|---|---|---|---|---|---|---|---|
| Mn10_143 | 286 | 173.1 ± 107.2 | 49.5 ± 43.8 | 1.4 ± 0.5 | -54.3 ± 30.1 | -32.6 ± 15.3 | 2.9 ± 7.1 | 62.4 ± 47.3 | 25.7 ± 13.6 | 11.7 ± 18.2 |
| Mn10_144 | 342 | 140.8 ± 70.9 | 52.5 ± 26.1 | 1.6 ± 0.3 | 33.2 ± 14.9 | -55.9 ± 19.3 | 4.7 ± 8.6 | 41.3 ± 24.2 | 41.0 ± 14.6 | 2.8 ± 9.1 |
| Mn10_146 | 88 | 469.5 ± 147.6 | 192.5 ± 102.8 | 1.5 ± 0.3 | 119.1 ± 47.6 | -56.6 ± 22.6 | 28.4 ± 9.7 | 143.0 ± 60.8 | 45.1 ± 26.1 | 43.6 ± 18.1 |
| Mn10_151 | 265 | 191.1 ± 103.7 | 56.8 ± 41.2 | 1.4 ± 0.4 | 53.2 ± 26.6 | -44.2 ± 22.4 | 37.9 ± 31.6 | 68.8 ± 38.0 | 29.8 ± 17.7 | 36.5 ± 33.1 |
| Mn10_155a | 153 | 288.1 ± 179.9 | 119.3 ± 122.1 | 1.4 ± 0.4 | 96.1 ± 73.3 | -44.0 ± 21.1 | 7.9 ± 9.8 | 96.4 ± 69.6 | 29.3 ± 27.6 | 32.6 ± 26.3 |
| Mn10_155b | 246 | 184.2 ± 151.5 | 58.0 ± 77.1 | 1.6 ± 0.5 | 63.9 ± 64.3 | -28.5 ± 10.8 | 5.0 ± 9.3 | 46.5 ± 43.8 | 23.1 ± 13.6 | 8.1 ± 12.4 |
| *ALL* | *3682* | *199.7 ± 150.1* | *64.0 ± 67.2* | *1.5 ± 0.4* | *58.6 ± 46.8* | *-39.8 ± 20.6* | *12.6 ± 20.0* | *68.1 ± 57.8* | *30.6 ± 22.4* | *18.8 ± 25.1* |

370    Mean ± standard deviation were shown. Dataset shaded with grey were not used for the Bayesian estimation due to insufficient number of 5-s

371    glides in the dataset.

372

373    Twenty-four of the 33 tag datasets (10 from the Gulf of St Lawrence and 14 from Antarctica)

374    were used to estimate tissue density and the other unknown parameters. Of the 12 Bayesian

375    models, the model with the lowest DIC indicated global plus individual variation in tissue

376    density and drag terms, and global plus dive-by-dive variability in diving lung volume (Table

377    3). The difference in DIC from the next-best model was 1657.5 units.

378

**Table 3. Model parameter values.**

| Model fit | Model structure | | | Global parameter estimates | | | | | |
|---|---|---|---|---|---|---|---|---|---|
| DIC | $\rho_{tissue}$ | $C_DAm^{-1}$ | $V_{air}$ | $\rho_{tissue}$.g | $\rho_{tissue}$.var | $C_DAm^{-1}$.g | $C_DAm^{-1}$.var | $V_{air}$.g | $V_{air}$.var |
| 28301.1 | I | I | D | 1031.6 (2.1) | 26.5 (17.2) | 11.8 (1.6) | 23.2 (16.4) | 27.7 (1.1) | 236.5 (33.4) |
| 29958.6 | I | G | D | 1031.3 (2.1) | 25.4 (16.2) | 11.6 (0.1) | | 26.5 (1.1) | 199.8 (25.6) |
| 53399.8 | G | I | D | 1029.4 (0.02) | | 7.9 (3.2) | 349.8 (369.6) | 21.0 (1.4) | 353.2 (57.2) |
| 86274.2 | G | G | D | 1029.7 (0.02) | | 8.3 (0.1) | | 20.7 (1.5) | 502.8 (89.2) |
| 106380.0 | I | I | I | 1030.3 (1.8) | 19.8 (11.8) | 8.5 (2.5) | 103.8 (86.0) | 25.7 (7.2) | 305.2 (288.2) |
| 113957.5 | I | G | I | 1030.1(1.7) | 17.3 (11.1) | 9.3 (0.1) | | 23.5 (5.8) | 193.1 (170.0) |
| 120768.9 | I | I | G | 1029.0 (1.1) | 6.5 (4.1) | 6.7 (1.8) | 39.7 (26.7) | 15.6 (0.1) | |
| 125832.6 | G | I | I | 1029.0 (0.02) | | 7.3 (3.2) | 215.5 (240.8) | 19.3 (6.5) | 227.8 (238.8) |
| 130603.2 | I | G | G | 1029.2 (1.13) | 7.4 (4.5) | 7.9 (0.1) | | 15.9 (0.1) | |
| 159607.6 | G | G | I | 1029.2 (0.01) | | 6.9 (0.1) | | 24.5 (17.0) | 1515.3 (2882.9) |
| 264515.3 | G | I | G | 1028.1 (0.01) | | 6.7 (3.5) | 1930.7 (7548.2) | 8.6 (0.1) | |
| 309390.4 | G | G | G | 1028.0 (0.01) | | 1.3 (0.04) | | 7.2 (0.1) | |

Model structure refers to the allowed variation in the model for the unknown terms, with G referring to global (i.e. individual-average) parameter only, I referring to individual specific estimates included, and D referring to dive-by-dive variation included. The column head refer to $\rho_{tissue}$ as tissue density (kg m$^{-3}$); $C_DAm^{-1}$ as combined drag term (m$^2$ kg$^{-1}$); $V_{air}$ as volume of air (ml kg$^{-1}$). Data are presented with ±95% CI in parentheses. For global parameter estimates, .g refers to the global parameter and .var refers to individual or dive-by-dive variance.

385 The global body tissue density was estimated with a posterior 95% credible interval (CI) of

386 1029.5 – 1033.6 kg m$^{-3}$ (mean = 1031.6 kg m$^{-3}$). Individual posterior mean values ranged

387 from 1025.2 to 1043.1 with ±95% CI of 0.04 – 2.3 kg m$^{-3}$.  The 95% CI range for individual

388 tissue density estimates decreased with increasing number of 5-s sub-glides in the dataset

389 （Fig. 1b). There was no significant relationship between the 95% CI range and the average

390 depth at which the sub-glides occurred (Spearman's rank test, p = 0.22); depth of glides

391 ranged from 5.1 to 343.2 m with individual mean ranging 25.2 ± 10.8 to 97.3 ± 55.4 m.  There

392 was a tendency for the 95% CI ranges to be smaller for the whales tagged in Antarctica using

393 DTAGs (0.6 ± 0.66 kg m$^{-3}$) than in the Gulf of St Lawrence using 3MPD3GTs (2.4 ± 1.11 kg

394 m$^{-3}$). It is possible that different sampling frequencies and resolution of sensors as well as

395 speed determination methods (measured/estimated) of 3MPD3GTs and DTAGs might

396 influence the precision of tissue density estimates. Yet, the effect of the two different archival

397 tag models could not be fully addressed due to the differences in location itself and longer

398 data duration for the Antarctic DTAG dataset (22.9 ± 1.6 h) compared to the Gulf of St

399 Lawrence 3MPD3GT dataset (3.5 ± 1.5 h; Table 1).

400

401 Whales in the Gulf of St Lawrence had relatively higher tissue density (median = 1034.0 kg

402 m$^{-3}$, range = 1026.5 – 1043.1 kg m$^{-3}$) than Antarctic whales (median = 1029.0 kg m$^{-3}$, range =

403 1025.2 – 1040.8 kg m$^{-3}$) although there was high inter-individual variation within each

404 feeding population (Fig. 2). The posterior mean tissue density of the male Mn11_H607 that

405 was tagged twice in July and September 2011 in the Gulf of St Lawrence decreased by 5.8 kg

406 m$^{-3}$ in 40 days (Table 1). Tissue densities of two pregnant females were estimated as the

407 lowest (1026.5 ± 0.5 kg m$^{-3}$ for Mn11_H002) and the second lowest (1028.6 ± 0.7 kg m$^{-3}$ for

408 Mn11_H584_2) among the whales from the Gulf of St Lawrence (Table 1). There was a

409 significant negative correlation between relative tissue density to seawater and percent time

410  spent gliding during ascent vs decent phases of non-feeding dives (Spearman's rho = -0.72, p

411  <0.001; Fig. 3).



412
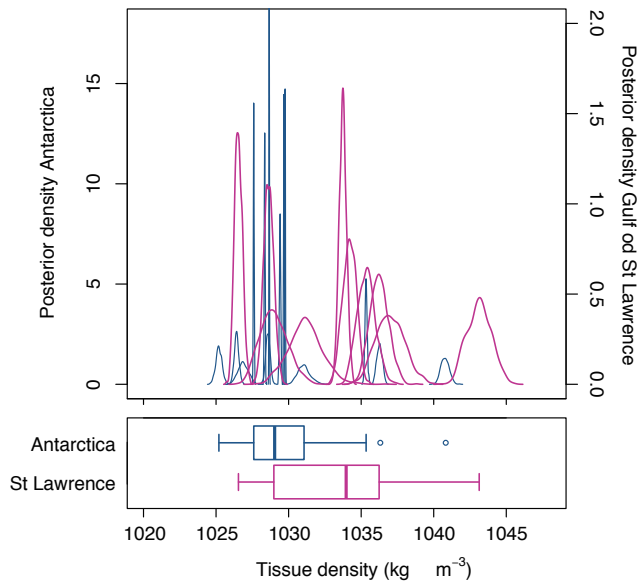
**Fig. 2 Tissue density estimates from the best model with the lowest DIC.** The top panel

shows posterior distribution of individual body tissue density for each tag deployment. Blue

and magenta lines indicate whales from Antarctica and the Gulf of St Lawrence, respectively.

Box plots in the bottom panel show median and interquartile range of tissue density estimates

from each location.
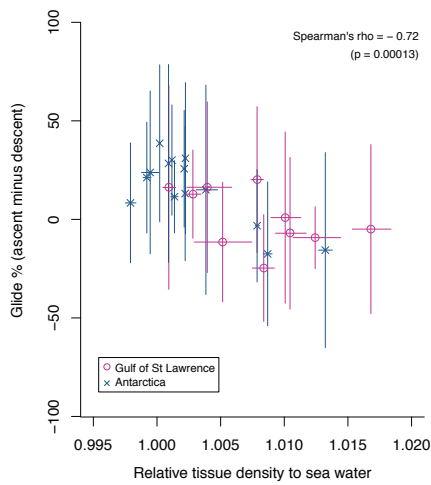


418

419 **Fig. 3 Relationship between gliding patterns and relative tissue density.** The y-axis

420 indicates differences in the percentage of time spent gliding during ascent and descent phases

421 of non-feeding dives by each whale. Vertical and horizontal error bars show standard

422 deviation and 95% credible interval range, respectively. A relative tissue density of >1

423 indicates that tissue density was denser than surrounding seawater.

424

425

426 The posterior mean of the global drag term was $11.8 \times 10^{-6} \pm 1.6 \times 10^{-6}$ $m^2$ $kg^{-1}$ ($\pm$ 95% CI).

427 The posterior mean was higher and the distribution had little overlap with the prior

428 distribution that had a mean of $7.0 \times 10^{-6}$ $m^2$ $kg^{-1}$ (Fig. 4). The posterior means of individual

429 drag term values ranged from $6.0 \times 10^{-6}$ to $25.5 \times 10^{-6}$ $m^2$ $kg^{-1}$, but most of them were near

430 $12.5 \times 10^{-6}$ $m^2$ $kg^{-1}$ (Table 1). The posterior mean of global diving gas volume was $27.7 \pm 1.1$

431 ml $kg^{-1}$ ($\pm$95% CI).

432

433 The best-fitting model with the lowest DIC evaluated dive-by-dive variation in diving gas

434 volume. The dive-by-dive estimates of diving gas volume ranged from 0.03 to 129.2 ml $kg^{-1}$,

435 but 90% of the estimates were within 9.2 – 53.5 ml $kg^{-1}$. Diving gas volume was estimated

436 slightly higher for feeding dives with more than 1 lunge (median = 26.3 ml $kg^{-1}$, range = 2.6 –

437 110.8 ml $kg^{-1}$) than other dives (median = 21.3 ml $kg^{-1}$, range = 0.8 – 97.5 ml $kg^{-1}$; Wilcoxon

438 rank sum test, p =0.021). Weak correlations between diving gas volume and dive depth were

439 observed for both feeding (Spearman's rho = 0.09, p = 0.036, N = 515) and non-feeding dives

440 (Spearman's rho = 0.21, p < 0.001, N = 252). However, no apparent relationships between

441 diving gas volume and dive duration were observed for feeding (Spearman's rho = 0.02, p =

442 0.58, N = 515) or non-feeding dives (Spearman's rho = 0.05, p = 0.45, N = 252).
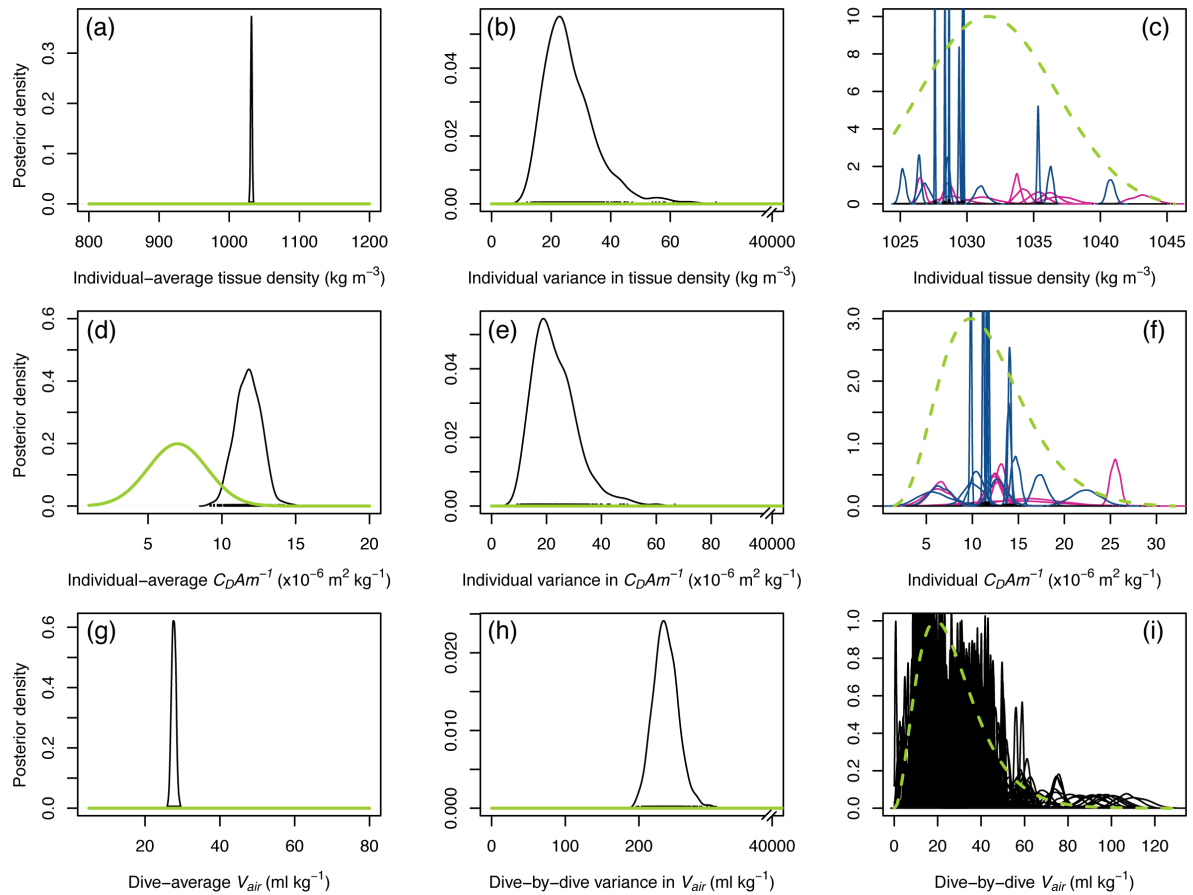
**Fig. 4 Prior and posterior distributions from the model with lowest DIC (Table 3).** Prior and posterior distributions of tissue density (a, b, c), drag term (d, e, f) and diving gas volume (g, h, i) are shown in each panel. Solid green and black lines indicate the prior and posterior distributions, respectively. Dashed green lines show the estimated global distribution that can be interpreted as the population distribution for that parameter. The left and middle panels show global parameters (a, b, d, e, g, h) and the right parameters show individual and dive-specific parameters.

# Discussion

To date, the hydrodynamic glide model has been used to estimate tissue density of deep diving marine mammals such as elephant seals, sperm whales, northern bottlenose whales and

456    long-finned pilot whales [15, 34, 38, 47]. In this study, we successfully applied this method to

457    substantially shallower-diving humpback whales to estimate tissue density from two

458    geographically distinct feeding populations. To examine the variability of the unknown

459    parameters (tissue density, drag and diving gas volume), we fitted 12 models with different

460    model structures. The best model included individual variation in tissue density and drag,

461    supporting our expectation that each whale had different tissue density. The best-fitting model

462    also included dive-by-dive variation in diving gas volume. Although there was no apparent

463    overall relationship between diving gas volume and dive duration, it is possible that whales

464    change the amount of inhaled air before dives depending on their activity [15].  The gliding

465    patterns of whales correlated with their estimated tissue density, with denser whales spending

466    relatively more time gliding during descent and less-dense whales spending more timing

467    gliding during ascent phases (Fig. 3). The significant correlation of tissue density and gliding

468    patterns provides a degree of validation that the tissue density estimates, or at least their

469    relative values, were accurate.

470

471    **Drag term estimates**

472    The drag coefficient is one of the key parameters to estimate tissue density using the

473    hydrodynamic glide model. Following Miller et al. [15], the combined drag term ($C_D A m^{-1}$)

474    was estimated using a relatively narrow Gaussian prior that was determined based on

475    auxiliary published data in order to improve the precision of tissue density estimates.

476    However, the global (individual-average) estimate of the drag term in the best-fitting model

477    ($11.8 \times 10^{-6}$ $m^2$ $kg^{-1}$) did not concentrate within the distribution of the prior ($7.0 \times 10^{-6}$ $m^2$ $kg^{-1}$

478    $^{1}$).

479

480   As in previous studies [15, 34, 38], we neglected any specific effect of lift, although lift-

481   related induced drag may not be negligible in the case of humpback whales due to their large

482   pectoral flippers [48] and propensity to glide at shallow angles. It is possible that the influence

483   of induced drag due to lift generation may explain the mismatch of the prior expectation of

484   the combined drag term and its posterior estimate from the data. Adding the induced drag to

485   the hydrodynamic glide model, the drag part of the equation can be expressed as

$$-0.5\rho_{sw}\frac{C_D A}{m}v^2 - 0.5\rho_{sw}\frac{A_{Flipper}}{\pi AR}\frac{C_L^2}{m}v^2$$

486   where $A_{Flipper}$ is flipper surface area (m$^2$), $AR$ is flipper aspect ratio and $C_L$ is the lift

487   coefficient [59]. Because both the parasite drag and the induced drag are a function of speed-

488   squared, the equation can be rewritten as

$$-0.5\rho_{sw}\left(\frac{C_D \cdot A}{m} + \frac{A_{Flipper}}{\pi \cdot AR}\cdot\frac{C_L^2}{m}\right)v^2$$

489   Thus, the structure of the equation is unchanged just with the addition of induced drag to that

490   of the parasite drag term $C_D A m^{-1}$.

491

492   We suggest that the model estimated higher global $C_D A m^{-1}$ values due to the effect of induced

493   drag by assuming that the model estimated the combined term in parenthesis, instead of the

494   parasite drag term ($C_D A m^{-1}$) alone. The lift coefficient of a humpback whale flipper is

495   estimated as $0 - 0.9$ through wind tunnel measurements [60]. Based upon literature values for

496   the surface area ($A_{Flipper}$, 12.20 m$^2$) and the aspect ratio ($AR$, 5.67) of a humpback whale

497   flipper [48], $A_{Flipper}C_L^2/(\pi AR m)$ is estimated as $0 - 22 \times 10^{-5}$ for a 12-m long whale. Adding

498   this value to $7 \times 10^{-6}$ (i.e. mean of the $C_D A m^{-1}$ prior), the combined drag term in the

499   parenthesis is expected to range between $7 \times 10^{-6}$ and $29 \times 10^{-6}$ m$^2$ kg$^{-1}$ which overlaps with

500   the global drag term estimates in this study ($11.8 \times 10^{-6} \pm 1.6 \times 10^{-6}$ m$^2$ kg$^{-1}$, $\pm$ 95% CI). This

501     suggests that the mismatch between the prior and $C_DAm^{-1}$ estimates derived from the addition

502     of the induced drag and that lift-related drag forces should not be ignored for this species.

503

504     In comparison with deeper diving marine mammals in previous studies [15, 34], the effect of

505     lift seems particularly important for humpback whales that glide at shallower pitch angles

506     (Table 2) where lift generation increases with correspondingly greater induced drag.

507     Humpback whales have large flipper with a high aspect ratio that can produce lift forces to

508     support their acrobatic movements such as high-speed turning and banking that are associated

509     with feeding [48, 61]. In addition, the scalloped leading edge of their large flippers serves to

510     delay stall angles and increase lift [60, 62]. Recent studies using animal-borne video camera

511     reported that humpback whales also perform lift-generating flipper strokes for propulsion

512     during lunge feeding [63]. In our study, we only used data during stable glides (circular

513     variance of roll < 0.1) to minimize the influence of lift during maneuvering. However, the

514     influence of lift-induced drag is detectable in our dataset possibly because humpback whales

515     likely use their wing-like flippers to produce lift during stable glides at non-vertical pitch

516     angles. Yet, it is noteworthy that our general results about tissue density seem to be robust

517     because the model quantified the combined effect of parasite and induced drag. As a

518     sensitivity analysis, we refitted the model using a non-informative wide range prior for the

519     drag term instead of a narrow Gaussian prior. The resulting global average drag term was 13.1

520     x $10^{-6} \pm 2.4$ x $10^{-6}\,m^2\,kg^{-1}$ and global average tissue density was $1031.6 \pm 2.1$ kg m$^{-3}$, which

521     differed very little from the estimated values with a narrow prior. Similarly, individual tissue

522     density estimates were nearly identical to the result of our original model, supporting the

523     robustness of the tissue density estimates to the prior specification.  Thus, the general results

524     about tissue density seem to be robust because the model appears to have estimated a

525     reasonable value for the combined effect of parasite and induced drag.

526

## Body tissue density

528  Estimated individual-average (global) body tissue density of humpback whales (1031.6 ± 2.1

529  kg m$^{-3}$; Table 3) was similar to that of other cetaceans reported to date (1030.0 ± 0.8 kg m$^{-3}$

530  for *Physeter macrocephalus* [38]; 1031.5 ± 1.0 kg m$^{-3}$ for *Hyperoodon ampullatus* [15]),

531  indicating that non-gas body tissues are typically denser than seawater. However, long-finned

532  pilot whales were estimated to have even denser tissues of 1038.8 ± 1.60 kg m$^{-3}$ [47]. For

533  humpback whales in this study, a large variation was detected in individual-specific body

534  tissue density ranging from 1025.2 to 1043.1 kg m$^{-3}$, as we expected, because individual

535  tissue density at feeding grounds would change depending on factors such as age, sex,

536  reproductive status, prey availability and the number of days since arrival at the feeding

537  ground [4, 6, 18, 24]. In a study of fin whales conducted using Icelandic whaling data,

538  pregnant females had the highest rate of fattening during the feeding season as they increased

539  their total body energy content by nearly 80% [4]. A similar trend was reported for minke

540  whales (*Balaenoptera acutorostrata*) in Iceland: the blubber volume of pregnant females

541  almost doubled over the feeding season [24]. Using the hydrodynamic glide model, high

542  lipid-stores of two pregnant female humpback whales (Mn11_H002 and Mn11_H584_2) were

543  indicated by low tissue density estimates of 1026.5 kg m$^{-3}$ and 1028.6 kg m$^{-3}$ that were the

544  lowest and the second lowest, respectively, among all of the tagged whales in the Gulf of St

545  Lawrence. A decrease in tissue density over the feeding season due to accumulation of lipid

546  stores was also detected in this study: tissue density of a repeated sampled adult male

547  (Mn11_H607) decreased from 1037.0 to 1031.2 kg m$^{-3}$ in 40 days. Based on extrapolation

548  from elephant seals, the proportion of lipid content ($P_{lipid}$) corresponding to these tissue

549  densities of Mn11_H607 would be 36.3% and 39.0%, as determined from $\rho_{tissue} =$

550  $\rho_{lipid}P_{lipid} + \rho_{lipid\text{-}free}(1 - P_{lipid})$, where $\rho_{lipid}$ and $\rho_{lipid\text{-}free}$ are 900.7 and 1114.6 kg m$^{-3}$, respectively

551   [34]. Our results also showed that one of the two calves had low body tissue density of 1025.2

552   kg m$^{-3}$ (Mn10_155b) in agreement with general expectation that calves are more buoyant

553   because they deposit fat during the lactation period [64]. The other calf (Mn10_139a),

554   however, had relatively high tissue density of 1040.8 kg m$^{-3}$ that was supported by its gliding

555   pattern suggestive of negative buoyancy: the whale spent more time gliding during descent

556   (61.3%) than ascent (45.7%) phases of non-feeding dives (Fig. 5d). It is possible that

557   Mn10_139a had a poor body condition, reflecting its mother's poor condition indicated by its

558   relatively high body density (Mn10_139b, 1029.4 kg m$^{-3}$) compared to the other mother in the

559   study (Mn10_155a, 1027.6 kg m$^{-3}$).

560   During the feeding season, it is essential for humpback whales to accumulate a sufficient

561   amount of energy for survival, growth and/or reproduction. Previous studies estimated the

562   amount of energy gained by baleen whales over the course of a feeding season via anatomical

563   measurements and chemical analysis of multiple whale carcasses  [4, 21]. More recent work

564   has described dynamic foraging patterns of whales throughout the course of the foraging

565   season suggesting that whales alter their feeding behaviour (rates and dive depth)

566   commensurate with changes in the availability of prey [65]. This could lead to non-linear

567   changes in the accumulation of energy, and, combined with body density estimates collected

568   over similar time periods, can offer insights as to the most critical times and locations for

569   whales to regain energy stores and how different life history classes vary.  This information is

570   critical to understanding how environmental changes and potential human disturbance can

571   significantly impact individual and population-level health of marine mammals and other

572   animals.

573
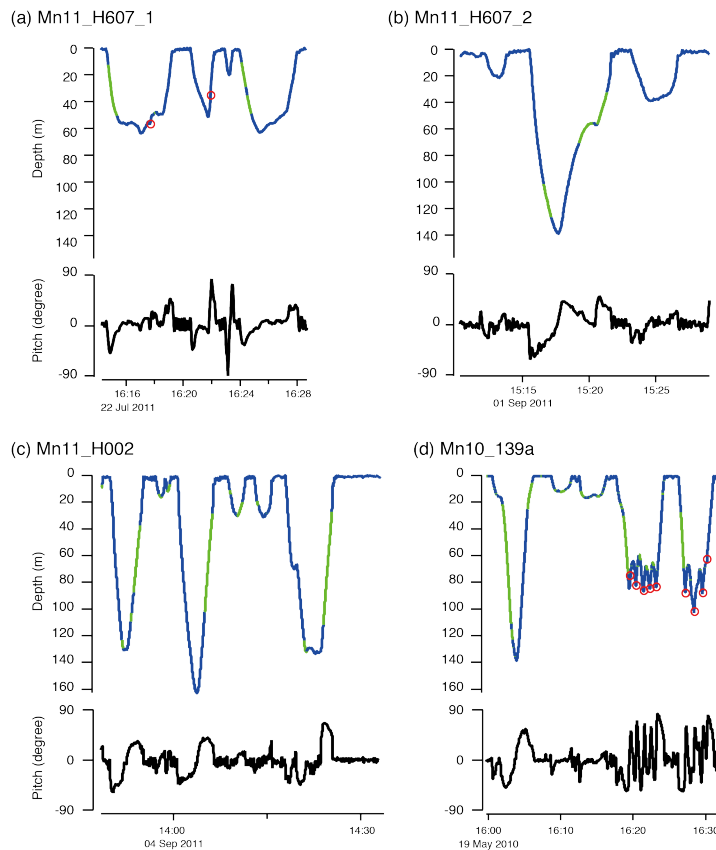
**Fig. 5 Example data records for dive profile and pitch.** Dive profile with gliding and stroking periods are indicated in green and blue, respectively. Red circles indicate feeding events. Examples are taken from an adult male during (a) early feeding season (tissue density = 1037.0 kg m$^{-1}$) and (b) late feeding season (1031.2 kg m$^{-1}$), (c) a pregnant female (1026.5 kg m$^{-1}$) and (d) a calf (1040.8 kg m$^{-1}$).

Changes in tissue density lead to changes in buoyancy that influence swimming patterns of diving animals given strong selection for them to travel efficiently to and from depth [33, 39]. For example, it is expected that animals with higher density should glide more during descent aided by negative buoyancy whereas less dense positively buoyant animals should employ more glides during ascent. In agreement with the expectation, a negative correlation between tissue density estimates and percent time spent gliding during ascent vs. descent phases of non-feeding dives was observed (Fig. 3), suggesting that the model successfully detected

588 relative differences in individual tissue density. Because there is greater variability in tissue

589 density of humpback whales than deep diving toothed whales [15, 38, 54], the relatively low

590 precision of tissue density estimates obtained here (±95% CI of individual tissue density

591 ranged up to 2.3 in this study whereas to 0.4 in [15]) seem to be sufficient to detect individual

592 and/or temporal variation. Lower precision tissue density estimates may be expected if there

593 is high variability in acceleration that is not accounted for in the model. Therefore, sample

594 size is particularly important to consider for the body density estimation of humpback whales

595 for which induced drag may cause variability in gliding acceleration. The result showed that

596 the number of 5-s sub-glides in each dataset is one of the key factors affecting the range of

597 95% CI for the posterior estimates of individual tissue density. Specifically for humpback

598 whales, >200 sub-glides in each dataset seem to be needed to obtain highly precise estimates

599 with 95% CI range of 1 kg m$^{-3}$ (Fig. 1b).

600

601  In this study, we estimated tissue density of humpback whales at two geographically distinct

602 feeding grounds. Tissue density of whales from Antarctica and Gulf of St Lawrence largely

603 overlapped, but there was a tendency for Antarctic whales to have lower tissue density (Fig.

604 2), indicating that animals in that location at that time had larger lipid reserves than did the

605 animals tagged in Canada. It is possible that the geographic differences reflected different

606 temperature and prey conditions on two feeding grounds. However, as numerous factors can

607 affect individual tissue density, more data, including basic information of individuals such as

608 sex, age class and reproductive status that can be obtained from photo-ID and biopsy studies

609 would be essential to identify factors that cause these geographic differences.

610

611 The methods used in this study closely followed methods published for other deep-diving

612 odontocete species.  Some studies used an estimated value of 0.06 for the entrained mass of

613    water $m_e$ which is moved forward along with the body of the animal [38]. Because we did not

614    have specific measurements of animal mass in this study, we also did not include estimates

615    for entrained mass. We also do not expect addition of a constant mass proportion of mass to

616    all estimates would affect their relative values. However, the absolute values obtained in this

617    study could be made more accurate with finer estimates of the length, mass and surface area

618    of each whale as was done using photogrammetry by Miller et al. [38]. We do recommend

619    incorporation of such data when available, and to include estimates of entrained mass to

620    obtain accurate absolute values of tissue body density.

621

## Diving gas volume

623    The posterior mean of global (dive-average) diving gas volume was $27.7 \pm 1.1$ ml kg$^{-1}$ ($\pm 95\%$

624    CI). This value is substantially lower than the estimated lung volumes of mysticete fin (29 –

625    61 ml kg$^{-1}$) and sei (*Balaenoptera borealis*) whales (116 – 151 ml kg$^{-1}$), whose lung volumes

626    were measured via inflation of excised lungs [66, 67]. This could indicate that: 1) lung

627    volumes of mysticete whales are smaller than estimated from excised lungs in which some

628    amount of air is likely to be trapped [46]. Piscitelli et al. [67] noted that the mass specific

629    volume of sei whales from that study were outliers on a comparative basis relative to smaller

630    cetaceans; 2) humpback whales in this study dove with less than their full lung capacity; or 3)

631    our estimate was incorrect and too low.

632

633    As cetaceans appear to inhale immediately prior to diving, the diving volume of cetaceans is

634    thought to be close to the total lung volume [68]. In fact, the calculated diving lung volume of

635    deep-diving northern bottlenose whales (27 ml kg$^{-1}$, [15]) was similar to the measured total

636    lung volume of 28 ml kg$^{-1}$ ([69] reviewed in [68]). However, shallower diving species may

637    not always dive with full lungs; for example, the diving lung volume and the total lung

638     volume of bottlenose dolphins are 40-50 ml kg$^{-1}$ [70] and 50-91 ml kg$^{-1}$, respectively

639     (reviewed by [67]). Differences in lung sizes and thoracic morphology of shallow and deep

640     diving cetaceans have been reported [46]. As the effect of air-derived buoyancy is stronger at

641     shallower depth, it is possible that shallower-diving whales do not always dive with full lung

642     capacity. A large variation in dive-by-dive estimates of diving gas volume found in this study

643     and, albeit weak, the positive relationship between diving gas volume and dive depth would

644     support this hypothesis. While no systematic variation of diving gas volume in relation to dive

645     duration was detected, further detailed analysis of dive-by-dive variation in diving gas volume

646     could provide new insights into their diving physiology.

647

648     Another possible explanation for the low estimate of diving gas volume is that the amount of

649     gas stored in the body might decrease during dives. It has been reported that humpback

650     whales actively exhale underwater in some situations. For example, humpback whales have a

651     diverse repertoire of feeding behaviours, including "bubble feeding" that involves underwater

652     exhalation to form bubble clouds, nets or curtains to corral prey [61, 71]. Bubbling is also

653     observed in non-feeding situations such as play [71] and social interactions [72]. Although

654     apparent bubbling was not detected from acoustic audits of the DTAG datasets in this study, it

655     is possible that some air might passively escape from the body during dives.. If such

656     underwater exhalation and/or passive loss of air occurred, our estimate of diving gas volume

657     would be too low because the majority of the glides used in the analysis were recorded during

658     ascent phases of dives, and thereby the estimate reflects the amount of gas in the body at latter

659     part of dives.

660

661     **Conclusion and future directions**

662    We demonstrated that the hydrodynamic glide model can be used to detect individual and

663    temporal variation in body tissue density of humpback whales, suggesting that it is likely to

664    be broadly applicable across a range of aquatic animals including shallow diving baleen

665    whales. The important next step is validation with other techniques such as visual assessment

666    [28, 29], biopsy sample measurements, and photogrammetric measurements of body width

667    versus length using overhead images [11, 30].

668

669    This study represents a cross-sectional design, in which the tissue densities of multiple

670    animals were measured.  Longitudinal tracking of changes in individuals' tissue density as has

671    been done with elephant seals drift dives [5], or repeated measurements as we made for whale

672    Mn11_H607, may be a more powerful approach to determine specific factors that affect the

673    lipid-store body condition of humpback whales. Considering that humpback whales are less

674    difficult to tag such that multiple tagging of the same individual is possible, this tag-based

675    minimally invasive approach may provide an effective tool to monitor body tissue density as a

676    measure of body condition. By integrating life-history data of individuals (e.g. age, sex, size,

677    reproductive status) as well as prey availability at feeding grounds, this approach can be

678    helpful to understand bioenergetics and health of individual whales within increasingly

679    human-altered ecosystems.   Ultimately, tracking the tissue density of individual whales using

680    longer duration tags could be a powerful technique to relate their body condition to how they

681    interact with features of their natural environment.

682

683

# **Acknowledgements**

684

687 to thank to all staffs and volunteers in Mingan Island Cetacean Study for field data collection.

688 We also thank the scientific and technical staff on the Antarctic cruises, particularly those

689 involved with tagging and tag data processing: Alison Stimpert, Ann Allen.

690

691 # References

692 1. Heithaus MR, Frid A, Wirsing AJ, Dill LM, Fourqurean JW, Burkholder D, Thomson J,

693     Bejder L. State-dependent risk-taking by green sea turtles mediates top-down effects of

694     tiger shark intimidation in a marine ecosystem. J Anim Ecol. 2007; 76: 837-844.

695 2. Bêty J, Gauthier G, Giroux J. Body condition, migration, and timing of reproduction in

696     snow geese: a test of the condition-dependent model of optimal clutch size. Am Nat.

697     2003; 162: 110-121.

698 3. Crossin GT, Phillips RA, Wynne-Edwards KE, Williams TD. Postmigratory body

699     condition and ovarian steroid production predict breeding decisions by female gray-

700     headed albatrosses. Physiol Biochem Zool. 2013; 86: 761-768.

701 4. Vikingsson GA. Body condition of fin whales during summer off Iceland. Developments

702     in Mar Biol. 1995; 4: 361-369.

703 5. Biuw M, McConnell B, Bradshaw CJA, Burton H, Fedak MA. Blubber and buoyancy:

704     monitoring the body condition of free-ranging seals using simple dive characteristics.  J

705     Exp Biol. 2003; 206: 3405-3423.

706 6. Williams R, Vikingsson GA, Gislason A, Lockyer C, New L, Thomas L, Hammond PS.

707     Evidence for density-dependent changes in body condition and pregnancy rate of North

708     Atlantic fin whales over four decades of varying environmental conditions. ICES J Mar

709     Sci. 2013; 70: 1273-1280.

710 7. Christiansen F, Vikingsson GA, Rasmussen MH, Lusseau D. Female body condition

711     affects foetal growth in a capital breeding mysticete. Funct Ecol. 2014; 28: 579 - 588

712    8.    Pomeroy PP, Fedak MA, Anderson SS, Rothery P. Consequences of maternal size for

713          reproductive expenditure and pupping success in grey seals at North Rona, Scotland. J

714          Anim Ecol. 1999; 68: 235-253.

715    9.    McMahon CR, Burton HR, Bester MN. Weaning mass and the future survival of

716          juvenile southern elephant seals, *Mirounga leonine*, at Macquarie Island. Antarct Sci.

717          2000; 12: 149-153.

718    10.   Hall AJ, McConnell BJ, Barker RJ. Factors affecting first-year survival in grey seals and

719          their implications for life history strategy. J Anim Ecol. 2001; 70:138-149.

720    11.   Christiansen F, Dujon AM, Sprogis KR, Arnould JPY, Bejder L. Noninvasive unmanned

721          aerial vehicle provides estimates of the energetic cost of reproduction in humpback

722          whales. Ecosphere. 2016; 7: 1 – 18.

723    12.   Friedlaender AS, Tyson RB, Stimpert AK, Read AJ, Nowacek DP. Extreme diel

724          variation in the feeding behaviour of humpback whales along the western Antarctic

725          Penninsula during autumn. Mar Ecol Prog Ser. 2014; 494:281-239.

726    13.   Friedlaender AS, Johnston DW, Tyson RB, Kaltenberg A, Goldbogen JA, Stimpert AK,

727          Curtice C, Hazen EL, Halpin PN, Read AJ, Nowacek DP. Multiple-stage decisions in a

728          marine central-place forager. P Soc Open Sci. 2016; 3: 160043.

729    14.   Stevenson RD, Woods WA Jr. Condition indices for conservation: new uses for evolving

730          tools. Integr Comp Biol. 2006; 46: 1169-1190.

731    15.   Miller P, Narazaki T, Isojunno S, Aoki K, Smout S, Sato K. Body density and diving gas

732          volume of the northern bottlenose whale (*Hyperoodon ampullatus*). J Exp Biol. 2016;

733          219: 2458-2468.

734    16.   National Research Council (NRC). Approaches to understanding the cumulative effects

735          of stressors on marine mammals. Washington DC: The National Academies Press; 2017.

736          Available from: http://www.nap.edu/23479

737   17. Kasuya T. Overview of cetacean life histories: an essay in their evolution. Dev Mar

738       Biol. 1995; 4: 481-498.

739   18. Lockyer C. Body fat condition in Northeast Atlantic fin whales, *Balaenoptera physalus*,

740       and its relationship with reproduction and food resource. Can. J. Fish. Aquat. Sci. 1986;

741       43:142-147

742   19. Aguilar A, Borrell A. Patterns of lipid content and stratification in the blubber of in

743       whales (*Balaenoptera physalus*). J Mammal. 1990; 71: 544-554.

744   20. Konishi K. Characteristics of blubber distribution and body condition indicators for

745       Antarctic minke whales (*Balaenoptera bonaerensis*). Mammal Study. 2006; 31: 15-22.

746   21. Lockyer C. Evaluation of the role of fat reserves in relation to the ecology of North

747       Atlantic fin and sei whales. In: Huntley AC, Costa DP, Worthy GAJ, Castellini MA,

748       editors. Approaches to Marine Mammal Energetics. Special Publication No 1. Lawrence:

749       Society for Marine Mammalogy; 1987. pp. 183-203.

750   22. Næss A, Haug T, Nilssen EM. Seasonal variation in body condition and muscular lipid

751       contents in northeast Atlantic Mike whale *Balaenoptera acutorostrata*. Sarsia 1998; 83:

752       211-218.

753   23. Vikingsson GA. Energetic studies on fin and sei whales caught off Iceland. Rep. Int.

754       Whal. Commn. 1990; 40:365- 373.

755   24. Christiansen F, Vikingsson GA, Rasmussen MH, Lusseau D. Mike whales maximise

756       energy storage on their feeding grounds. J Exp Biol. 2013; 216: 427-436.

757   25. Lockyer CH, McConnel LC, Waters TD. Body condition in terms of anatomical and

758       biochemical assessment of body fat in North Atlantic fin and sei whales. Can J Zool.

759       1985; 63: 2328-2338.

760   26. Lambertsen RH. A biopsy system for large whales and its use for cytogenetics. J.

761       Mamm. 1987; 68: 443-445.

762 27. Ryan C, McHugh B, O'Connor I, Berrow S. Lipid content of blubber biopsies is not

763   representative of blubber in situ for fin whales (*Balaenoptera physalus*). Mar Mamm Sci.

764   2012; 29: 542-547.

765 28. Pettis HM, Rolland RM, Hamilton PK, Brault S, Kowlton AR, Kraus SD. Visual health

766   assessment of North Atlantic right whales (*Eubalaena glacialis*) using photographs. Can.

767   J. Zool. 2004; 82: 8-19.

768 29. Bradford AL, Weller, DW, Punt WAE, Ivashchenko YI, Burdin AM, VanBlaricom GR,

769   Brownell RL Jr. Leaner leviathans: body condition variation in a critically endangered

770   whale population. J Mammal. 2012; 93: 251-266.

771 30. Miller CA, Best PB, Perryman WL, Baumgartner MF, Moore MJ. Body shape changes

772   associated with reproductive status, nutritive condition and growth in right whales

773   *Eubalaena glacialis* and *E. australis*. Mar Ecol Prog Ser. 2012; 459: 135-156.

774 31. Durban JW, Moore MJ, Gustavo C, Hickmott LS, Bocconcelli A, Howes G, Bahamonde

775   PA, Perryman WL, LeRoi DJ. Photogrammetry of blue whales with an unmanned

776   hexacopter. Mar Mamm Sci. 2016; 32:1510-1515.

777 32. Moya-Laraño J, Macias-Ordóñez R, Blanckenhorn WU, And Fernández-Montraveta C.

778   Analysing body condition: mass, volume or density? J. Anim. Ecol. 2008; 77: 1099-

779   1108.

780 33. Williams TM, Davis RW, Fuiman LA, Francis J, LeBoeuf BJ, Horning M, Calambokidis

781   J, Croll DA. Sink or swim: strategies for cost-efficient diving by marine mammals.

782   Science. 2000; 288: 133-136.

783 34. Aoki K, Watanabe Y, Crocker DE, Robinson PW, Biuw M, Costa DP, Miyazaki N,

784   Fedak MA, Miller PJO. Northern elephant seals adjust gliding and stroking patterns with

785   changes in buoyancy: validation of at-sea metrics of body density. J Exp Biol. 2011;

786   214: 2973-2987.

787    35.   Richard G, Vacquié-Garcia J, Jouma'a J, Picard B, Génin A, Arnould JPY, Bailleu F,

788        Guinet C. Variation in body condition during the post-moult foraging trip of southern

789        elephant seals and its consequences on diving behaviour. J Exp Biol. 2014; 217: 2609-

790        2619.

791    36.   Nowacek DP, Johnson MP, Tyack PL, Shorter KA, McLellan WA, Pabst DA. Buoyant

792        balaenids: the ups and downs of buoyancy in right whales. Proc R Soc B. 2001; 268:

793        1811-1816.

794    37.   Sato K, Mitani Y, Cameron MF, Siniff DB, Naito Y. Factors affecting stroking patterns

795        and body angle in diving Weddell seals under natural conditions.  J Exp Biol. 2003; 206:

796        1461-1470.

797    38.   Miller PJO, Johnson MP, Tyack PL, Terray EA.  Swimming gaits, passive drag, and

798        buoyancy of diving sperm whales *Physeter macrocephalus*.  J Exp Biol. 2004; 207:

799        1953-1967.

800    39.   Watanabe Y, Baranov EA, Sato K, Naito Y, Miyazaki N. Body density affects stroke

801        patterns in Baikal seals.  J Exp Biol. 2006; 209: 3269-3280.

802    40.   Biuw M, Boehme L, Guinet C, Hindell M, Costa, D, Charrassin JB, Roquet F, Bailleul

803        F, Meredith M, Thorpe S, et al. Variations in behavior and condition of a Southern

804        Ocean top predator in relation to in situ oceanographic conditions. Proc. Natl. Acad. Sci.

805        2007; 104: 13705-13710.

806    41.   Robinson PW, Simmons SE, Crocker DE, Costa DP. Measurements of foraging success

807        in a highly pelagic marine predator, the northern elephant seal. J Anim Ecol. 2010; 79:

808        1146-1156.

809    42.   Crocker DE, Le Boeuf BJ, Costa DP. Drift diving in female northern elephant seals:

810        implications for food processing. Can. J. Zool. 1997; 75: 27–39. doi:10.1139/z97-004

811    43. Page B, McKenzie J, Goldsworthy SD. Inter-sexual differences in New Zealand

812          fur seal diving behaviour. Mar Ecol Prog Ser. 2005; 304: 249–264.

813    44. Andersen JM, Stenson GB, Skern-Maurizen M, Wiersma YF, Rosing-Asvid A, Hammill

814          MO, Boehme L. Drift diving by hooded seals (*Cystophora cristata*) in the Northwest

815          Atlantic Ocean. PLoS One. 2014. https://doi.org/10.1371/journal.pone.0103072

816    45. Reilly JJ, Fedak MA. Measurement of the body composition of living gray seals by

817          hydrogen isotope dilution. J Appl Physiol. 1990; 69: 885-891.

818    46. Piscitelli MA, McLellan WA, Rommel SA, Blum JE, Barco SG, Pabst DA. Lung size

819          and thoracic morphology in shallow- and deep-diving cetaceans. J Morphol. 2010; 271:

820          654-673.

821    47. Aoki K, Sato K, Isojunno S, Narazaki T, Miller PJO. High diving metabolic rate

822          indicated by high-speed ransit to depth in negatively buoyant long-finned pilot whales. J

823          Exp Biol. 2017; 220: 3802-3811.

824    48. Woodward BL, Winn JP, Fish FE. Morphological specializations of baleen whales

825          associated with hydrodynamic performance and ecological niche. J Morphol. 2006; 267:

826          1284-1294.

827    49. Johnson M, Tyack PL. A digital acoustic recording tag for measuring the response of

828          wild marine mammals to sound.  IEEE J Ocean Eng. 2003; 28: 3-12.

829    50. Shiomi K, Narazaki T, Sato K, Shimatani K, Arai N, Ponganis PJ, Miyazaki N. Data-

830          processing artefacts in three-dimensional dive path reconstruction from geomagnetic and

831          acceleration data. Aquat Biol. 2010; 8:299-304.

832    51. Goldbogen JA, Pyenson ND, Shadwick RE. Big gulps require high drag for fin whale

833          lunge feeding. Mar Ecol Prog Ser. 2007; 349: 289-301.

834   52.  Simon M, Johnson M, Madsen PT. Keeping momentum with a mouthful of water:

835        behaviour and kinematics of humpback whale lunge feeding. J Exp Biol. 2012; 215:

836        3786 – 3798.

837   53.  Bose N, Lien J. Propulsion of a fin whale (*Balaenoptera physalus*): why the fin whale is

838        a fast swimmer. Proc R Soc Lond B. 1989; 237:175-200.

839   54.  Lockyer C. Body weights of some species of large whales. J. Cons. Int. Explor. Mer.

840        1976; 36: 259-273.

841   55.  Fish FE. Power output and propulsive efficiency of swimming bottlenose dolphins

842        (*Tursiops truncates*). J Exp Biol. 1993 185: 179-193.

843   56.  Kooyman GL. Diverse Divers. Physiology and behaviour. Berlin: Springer-Verlag;

844        1989.

845   57.  Brooks SP, Gelman A. General methods for monitoring convergence of iterative

846        simulations. J. Comput. Graph, Stat. 1998; 7: 434-455.

847   58.  Ramp C, Delarue J, Palsbøll PJ, Sears R, Hammond PS. Adapting to a Warmer Ocean—

848        Seasonal Shift of Baleen Whale Movements over Three Decades. PLoS ONE, 2015; 10:

849        e0121374. doi: 10.1371/journal.pone.0121374

850   59.  Sato K, Naito Y, Kato A, Niizuma Y, Watanuki Y, Charrassin JB, Bost CA, Handrich Y,

851        Le Maho Y. Buoyancy and maximal diving depth in penguins: do they control inhaling

852        air volume? J Exp Biol. 2002; 205: 1189-1197.

853   60.  Miklosovic DS, Murray MM, Howle LE, Fish FE. Leading-edge tubercles delay stall on

854        humpback whale (*Megaptera novaeangliae*) flippers. Phys Fluids. 2004; 16: L39-L42.

855        doi: http://dx.doi.org/10.1063/1.1688341

856   61.  Wiley D, Ware C, Bocconelli A, Cholewiak D, Friedlaender A, Thompson M, Weinrich

857        M. Underwater components of humpback whale bubble-net feeding behaviour.

858        Behaviour. 2011; 148: 576-602.

859    62. Fish FE, Battle JM. Hydrodynamic design of the humpback whale flipper. J Morphol.

860          1995; 225: 51-60.

861    63. Segre PS, Seakamela SM, Meyer MA, Findlay KP, Goldbogen JA. A hydrodynamically

862          active flipper-stroke in humpback whales. Curr Biol. 2017; 27: R623-R641.

863    64. Miller CA, Reeb D, Best PB, Knowlton AR, Brown MW, Moore MJ. Blubber thickness

864          in right whales *Eubalaena glacialis* and *Eubalaena australis* related with reproduction,

865          life history status and prey abundance. Mar Ecol Prog Ser. 2011; 438: 267-283.

866    65. Weinstein B, Friedlaender AS. Dynamic foraging of a top predator in a seasonal polar

867          marine environment. Oecologia. 2017; 185: 427-435.

868    66. Leith D, Lowe R. Mechanics of baleen whale lungs. Fed Proc. 1972; 31: 335A

869    67. Piscitelli MA, Raverty SA, Lillie MA, Shadwick RE. A review of cetacean lung

870          morphology and mechanics. J Morphol. 2013; 274: 1425-1440.

871    68. Ponganis PJ. Diving mammals. Compr Physiol. 2011; 1: 447-465.

872    69. Scholander PF. Experimental investigations on the respiratory function in diving

873          mammals and birds. Hvalradets skrifter. 1940; 22: 1-131.

874    70. Skrovan RC, Williams TM, Berry PS, Moore PW, Davis RW. The diving physiology of

875          bottlenose dolphins (*Tursiops truncatus*), part II: Biomechanics and changes in buoyancy

876          at depth. J Exp Biol. 1999; 202: 2749-2761.

877    71. Hain JHW, Carter GR, Kraus SD, May CA, Winn HE. Feeding behaviour of the

878          humpback whale, *Megaptera novaeangliae*, in the western north Atlantic. Fish Bull.

879          1982; 80: 259-268.

880    72. Tyack P, Whitehead H. Male competition in large groups of wintering humpback

881          whales. Behaviour, 1983; 83: 132–154.

882

883

# Supporting Information

**S1 Fig. Examples of linear regression of speed over time to estimate acceleration during 5s sub-glides.** Linear regression of speed over time was conducted at each 5s sub-glide to estimate acceleration as a slope of the regression line. Top and bottom panels show examples from 3MPD3GT and DTAG deployments, respectively.

**S1 File. Data of all 5-s sub glides performed by tagged humpback whales.** This file includes all 5-s sub glides data used in this study.